ELSEVIER

Catalysis Today 83 (2003) 183–197

CATALYSIS TODAY

www.elsevier.com/locate/cattod

Complete and partial catalytic oxidation of methane over substrates with enhanced transport properties

Maxim Lyubovsky*, Hasan Karim, Paul Menacherry, Sam Boorse, Rene LaPierre, William C. Pfefferle, Subir Roychoudhury

Precision Combustion Inc., 410 Sackett Point Road, North Haven, CT 06473, USA

Received 1 May 2002; received in revised form 10 November 2002; accepted 18 March 2003

Abstract

The development of improved substrate properties for catalytic combustion has been an area of much interest in recent years. Towards this end, Precision Combustion Inc. has developed novel short channel length, high cell density substrates (trademarked Microlith®) and high surface area ceramic coatings for them. These substrates avoid substantial boundary layer buildup and greatly enhance heat and mass transfer rates in reactors. The high cell density of these substrates results in high amount of the catalyst per unit of reactor volume. In this paper we examine the performance of these substrates coated with precious metal catalysts for the catalytic combustion and reforming of methane.

Under fuel-lean operating conditions the surface temperature of Pd-based catalyst supported on Microlith® substrate and the temperature of the gas exiting the reactor remain stable at ∼800 °C over a wide range of inlet conditions. This is attributed to combination of enhanced transport properties and characteristics of Pd–PdO transformation. Preheating of the gas mixture in the Microlith® reactor was sufficient to stabilize a downstream premixed flame with NO_x, CO, and UHC emissions in the single digit ppm range.

Microlith® substrates were also examined for partial oxidation of methane under fuel-rich conditions. The enhanced transport properties of the Microlith® substrate allowed complete conversion of methane with surface temperature not exceeding material limits at 93% selectivity to partial oxidation products. High flow rate of reactants result in extremely high power densities and syngas output. The catalyst performance was observed to be stable over 500 h of operation.

Keywords: Mass transfer rate; Catalytic combustion; Partial oxidation; Syngas; Natural gas

1. Introduction

Natural gas is an abundant and relatively clean fuel with reserves that will last well into the 21st century. Developing effective technologies for the utilization of energy stored in natural gas has been the subject of much research both in academia and in industry. Methane, which is the principle component of natural gas, is one of the most difficult hydrocarbon molecules to oxidize [1]. Combustion of methane in homogeneous flames usually requires very high temperatures, where high levels of NO_x are produced. Stabilization of leaner, colder flame leads to drastic reduction in NO_x emissions and therefore, is one of main objectives in development of combustion processes.

* Corresponding author. Tel.: +1-203-287-3700; fax: +1-203-287-3710.
E-mail address: mlyubovsky@precision-combustion.com (M. Lyubovsky).

0920-5861/$ – see front matter © 2003 Elsevier B.V. All rights reserved.
doi:10.1016/S0920-5861(03)00231-1

Several technologies have been developed to achieve this objective, namely dry low NO_x (DLN) and catalytic combustion. However, DLN combustion systems only guarantee below 10 ppm NO_x emissions under limited operating range. It is well established that catalytic combustion can simultaneously achieve single digit NO_x, unburned hydrocarbons and CO emissions for operation with natural gas by stabilizing flames at temperatures, where thermal NO_x production is negligible. Lean premixed catalytic combustion of methane has been extensively studied and previous research has identified Pd-based catalysts as having the highest activity for methane combustion under these conditions. However, problems remain with the activity, stability, and durability of these systems.

Another challenge in natural gas utilization is transportation from remote areas, where many large reserves are found. Converting natural gas into higher hydrocarbons through gas-to-liquid (GTL) processes is considered to be an effective way of decreasing the transportation costs. In current GTL technologies the first step in which methane is converted into syngas (mixture of CO and H_2) constitutes about 60% of the overall cost. In recent years converting methane into syngas via catalytic partial oxidation has shown much promise. In this process, a fuel-rich mixture of methane with air or oxygen is passed over a catalyst at very high space velocity and is converted mainly into CO and H_2. However achieving high conversion of methane with high selectivity to partial oxidation products at low catalyst temperatures has been a challenge for this process.

In order to address these challenges an effective catalytic system was developed through the use of high specific surface area (SSA) coatings on novel short channel length, high cell density (Microlith®) substrates. This substrate technology comprises multiple metallic monoliths, having very small channel-length to channel-diameter ratio, minimizing channel boundary layer buildup and resulting in remarkably high heat and mass transfer coefficients compared to conventional monolith substrates. While noble metal gauze catalysts are widely used in chemical industry, for example in ammonia oxidation for nitric acid production, they are used in the form of bulk metal wire catalysts. This results in low surface area (essentially geometric area of the wire) and extremely high amount of precious metal loading and limits application of these catalysts beyond the few known chemical processes. On the other hand application of high surface area washcoats and highly dispersed catalysts to inexpensive metal wire screens provides a decisive decrease in precious metal usage without compromising the high mass and heat transfer properties of the mesh substrates. This allows utilization of these catalytic systems in multiple applications including catalytic combustion and fuel reforming.

2. Microlith® catalyst substrate technology

Typical parameters for monolith and Microlith® substrates are compared in Fig. 1. The geometry of the Microlith® substrate provides about three times higher geometric surface area (GSA) for supporting active catalyst materials over reactors (i.e. monolith) with equivalent volume and open frontal area. The greatest advantage of the Microlith® substrate, though, comes from the difference in boundary layer formation between a Microlith® and a conventional monolith as illustrated in Fig. 2. The predictions of the boundary layer development inside a monolith and a Microlith® substrates were generated using FLUENT, a commercially available CFD package. The predictions for monolith were made for a sample with 70% open area and 400 cpsi, and for Microlith® for a set of three 50 mesh (20 cells per linear cm) wire screens with wire diameter of 76 μm separated from each other by a distance of 6 wire diameters. For both cases bulk stream velocity was assumed at 6.1 m/s, which corresponds to Reynolds numbers of $Re = 110$ for the monolith and $Re = 6.5$ for the Microlith®. In calculating the Reynolds number for the Microlith®, the wire mesh diameter (d_w), was used as the characteristic length, as suggested by Sodre and Parise [2]. In both cases, a laminar flow solver was used as suggested by the Reynolds numbers. Fig. 2 shows the predictions of steady state axial velocities. To emphasize the difference in the boundary layer thickness between the two systems, bulk stream velocities are not shown and any axial velocity over 3 m/s was clipped. Thus, Fig. 2 shows that the boundary layer for a monolith substrate grows thicker as the length increases, whereas for a Microlith® substrate the boundary layer growth is very small and exist over a very short distance.

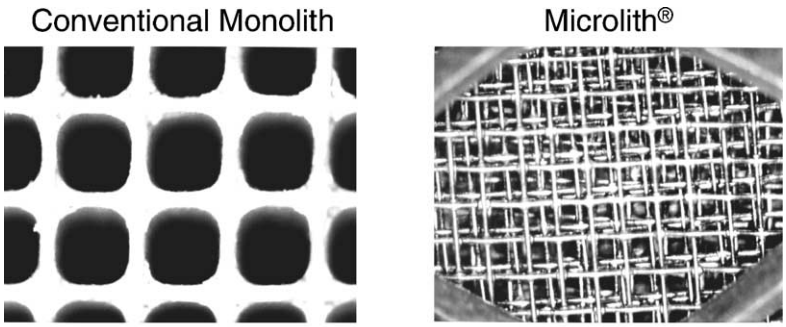

60	Cells/cm^2	400
2.64	Geometric Surface Area (m^2/liter)	6.3
7 - 10	Channel Length (cm)	0.007
70 - 120	Channel Length to Diameter Ratio (L/d)	0.3
1050 - 1200	Operating Temperature (C)	1050 - 1200
70	Frontal Open Area (%)	72

Fig. 1. Physical characteristics of conventional monolith and Microlith® substrates.

The heat and mass transfer coefficients depend on the boundary layer thickness. For a conventional long channel honeycomb monolith, a fully developed boundary layer will present over a considerable length of the catalytic surface, limiting the rate of reactant transport to the active sites. The Microlith® technology replaces long channel monoliths with a series of extremely short channel screens, each screen been shorter than the entrance region for the monolith, thus avoiding substantial boundary layer build-up. The effectiveness of the Microlith® technology has been demonstrated in various applications such as IC engine exhaust after treatment [3], trace contaminant control, [4] and catalytic combustion [5].

Ullah et al. [6] have developed an experimental correlation between mass transfer coefficients and the ratio of channel length to channel diameter (L/D) for ceramic monoliths by measuring mass transfer limited conversion over monoliths of various lengths and averaging the mass transfer coefficient (k_c) over the length of the monolith (shown graphically in Fig. 3 for a 350 cpsi ceramic monolith). An experimentally derived correlation by Satterfield and Cortez [7] for a short channel length monolith yields a mass transfer

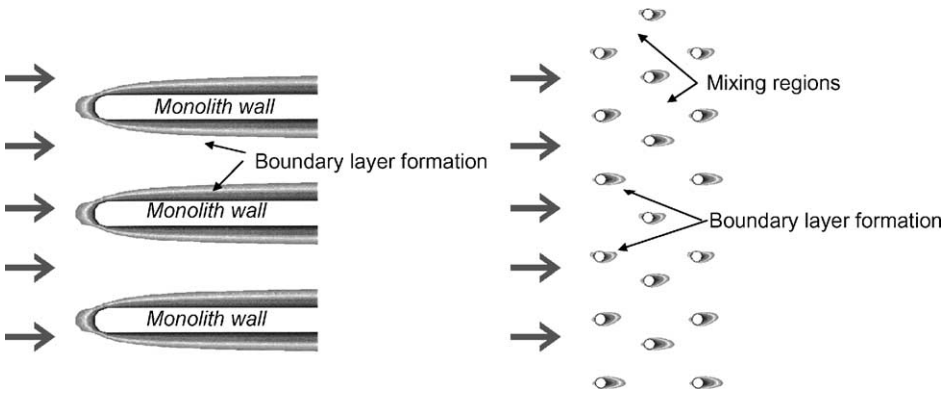

Fig. 2. CFD results of boundary layer formation for a conventional monolith and three Microlith® elements in series (6 m/s air at 450 °C).

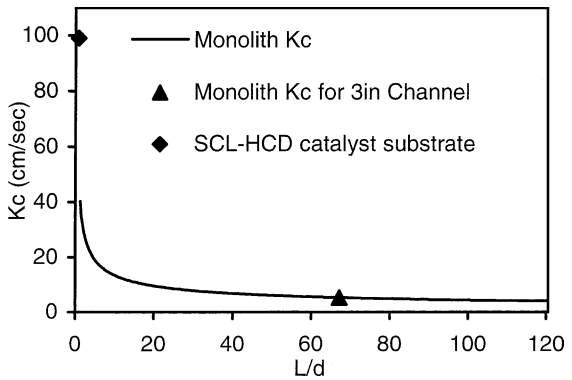

Fig. 3. Mass transfer coefficient comparison for Microlith® substrate and conventional monolith [6] (CO in air at 350 °C, velocity = 1.6 m/s).

coefficient of approximately 100 cm/s under similar conditions as shown in Fig. 3.

Fig. 4 shows a prediction of mass transfer coefficients as function of L/D ratio and flow velocity for monolith with a channel diameter of 3 mm. The mass transfer coefficients are determined by using Reynold's analogy between heat and mass transfer coefficients and correlation given for heat transfer coefficients in Shah and London [8]. Conventional monoliths have L/D ratio much greater than 10, whereas for Microlith® substrate this ratio is in the range of 0.1–0.5. From the Fig. 4, we observe that at gas turbine conditions (velocity > 30 m/s) reactors based on Microlith® substrate have substantially higher overall mass transfer coefficients than reactors based on monolith substrate. The 3D plot suggests that, while increasing the flow velocity over conventional monolith substrates does provide some increase in mass transfer rate, a similar increase can be obtained over the Microlith® substrate at much lower flow velocities. The data also suggest that, the higher the velocity is, the greater is the difference between the mass transfer coefficients for reactor based on monolith and Microlith® substrate. Higher mass transfer coefficients implies higher heat transfer coefficients. At a velocity of 50 m/s, the correlation predicts mass transfer coefficient of 228 cm/s for Microlith® substrate (L/D of 0.1) vs. 28 cm/s for conventional 1 in. long monolith substrate (L/D of ∼10).

Under mass transfer limited operation, conversion x, over a catalyst of area A is

$$x = 1 - \exp\left(-\frac{k_g A}{Q}\right) \tag{1}$$

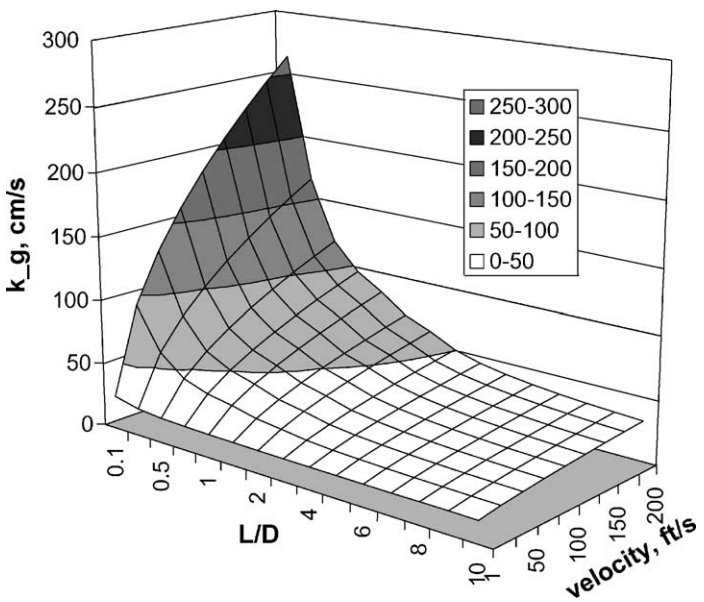

Fig. 4. Correlation between the channel length to diameter ratio, flow velocity, and the mass transfer coefficient between the gas and the catalyst. Calculations are made for monolith with channel diameter of 0.125 in.

where Q is the volumetric flow rate, k_g the mass transfer coefficient and A the total GSA. As discussed earlier Microlith® substrates have much higher mass transfer coefficients and from Eq. (1), we can see that this will result in much higher conversion for mass transfer limited reaction. Comparative tests of propylene combustion under equivalent conditions over a stack of Microlith® elements having a length of 0.11 cm and a ceramic monolith having a length of 2.54 cm were performed at PCI [9]. Equivalent conversion of propylene over both systems was observed under the mass transfer limited regime of operation, which agrees well with estimates from the mass transfer correlation of these substrates. Pressure drop for these two reactors was also found to be equivalent. The 20-fold decrease in reactor volume translates into a significant decrease in precious metal loading for the Microlith® reactor. The conversion per unit of substrate surface area can be up to an order of magnitude higher for the Microlith® than for the conventional monolith substrate. As loading of the catalyst material per unit of surface area for these substrates is about the same, a Microlith® reactor would require ten times less precious metal to provide similar conversion.

Porous catalyst washcoats on the two substrates were modeled using the Thiele Model for intraparticle diffusion [6], a bulk mass transfer rate based on the mass transfer coefficient (k_c) and a bulk gas phase concentration C of the reacting species. Note that this analysis considered a differential reactor, i.e. C was assumed constant over the length of the reactor. While the actual application will utilize an integral reactor, the results from the differential reactor are illustrative in that they show the effect of mass transfer coefficient on the observed reaction rate across a differential section of reactor. From this analysis:

$$C_s = \frac{k_g A C}{(\Phi D/L^2) + k_g A} \tag{2}$$

where C_s is the concentration of the reacting species i at the washcoat periphery, Φ the modified Thiele modulus, L a length parameter, in this case the washcoat thickness D is the effective diffusivity of the gas molecules in the pores and A is GSA per reactor. Therefore, the observed rate of reaction per reactor is given by the following expression:

Table 1
Parameters for Thiele analysis

Parameter	Microlith® catalyst substrate	Monolith (60 cell/cm^2)
k_c (m/s)	1.30	0.10
A (m^2)	0.37	3.46

$$\text{rate} = \frac{k_g A C}{1 + k_g A/(\Phi D/L^2)} \tag{3}$$

The parameters used to model the conventional monolith and the Microlith® substrates are shown in Table 1. The results of Eq. (3) for the Microlith® substrate and a 400 cpsi, 1 in. monolith substrate are plotted in Fig. 5.

It can be seen in Fig. 5 that, the parameter $\Phi D/L^2$ collapses data for different values of effective diffusivity D and washcoat thickness L, onto the same curve. From the Thiele model:

$$\frac{\Phi D}{L^2} = k\eta \tag{4}$$

where k is the intrinsic reaction rate and η the effectiveness factor (equal to the observed reaction rate divided by the reaction rate that would prevail in the absence of diffusion effects). The intrinsic reaction rate k, has an exponential dependence on temperature, whereas $\eta \sim 1$ for $\Phi < 1$. Therefore, the x-axis in Fig. 5 which is logarithmic in $(\Phi D/L^2)$ can be considered approximately linear in temperature.

This analysis shows that enhanced transport properties of the Microlith® substrate result in a delayed onset of mass transfer limited conversion compared to conventional long channel monolith reactors, and higher conversion for equivalent pressure drop and a fraction of the volume under mass transfer limited operation. The delayed onset of mass transfer limited conversion may be highly beneficial in catalytic combustion applications, wherein it is necessary to keep the reactor from running mass transfer limited, since the adiabatic flame temperature is well above the material limitations of the catalyst/substrate.

In order to capitalize on the inherent advantages of the Microlith® substrate high surface area (SSA) washcoats have been developed by creating a porous ceramic layer comprised of a ceramic powder and a ceramic binder which holds the powder together (washcoat cohesion) and the washcoat to the surface of the metal substrate (washcoat adhesion). Characteristics of the Microlith® geometry places stringent

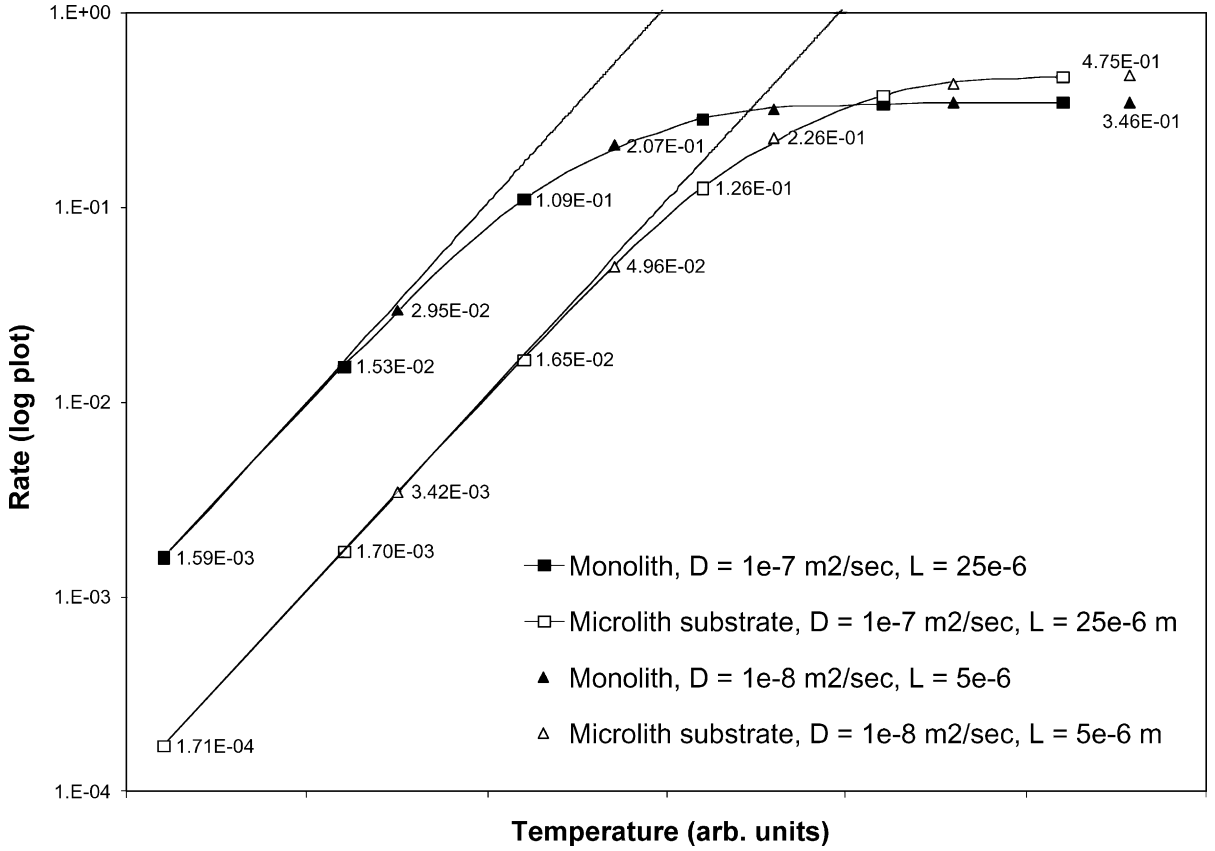

Fig. 5. Effect of mass transfer coefficient on observed reaction rates: Φ is the modified Thiele modulus, D the effective diffusivity of the gas molecules in the pores, and L the washcoat thickness. *Note*: this analysis compares a conventional 60 cell/cm^2 monolith with a Microlith® substrate reactor less than 1/10th of the size.

requirements on the properties of the high surface area ceramic washcoat for these systems. Ceramics have lower thermal expansion coefficient than the underlying metal, therefore elevated temperatures tend to put the ceramic coating under tension. This expansion mismatch is further exacerbated with decreasing radius of curvature. Because of the low tensile strength of ceramic materials, fracture is a major concern. While a conventional monolith, with 50–80 cells/cm^2 and aspect ratio (length to channel diameter, L/d) ~100, is essentially a flat surface in the axial direction, the Microlith® geometry has a surface with a radius of curvature comparable to the coating thickness. Therefore, a major achievement has been the development of adherent washcoats for these metal substrates. In addition to adhesion, another critical issue with the formation of washcoats on Microlith® substrate was surface area stability at high operating temperatures. Many conventional washcoat materials have very high surface areas at low temperature but sinter into much more dense phases at high temperature. Presence of water vapor in combustion gas atmospheres also greatly accelerates the loss of surface area at high temperatures. PCI has developed washcoat formulations that are stable in combustion applications at high temperatures by adding stabilizing elements to the ceramic powders.

3. Application of Microlith® substrate to fuel-lean catalytic combustion

In this section, we will discuss how the inherent properties of short channel length Microlith® sub-

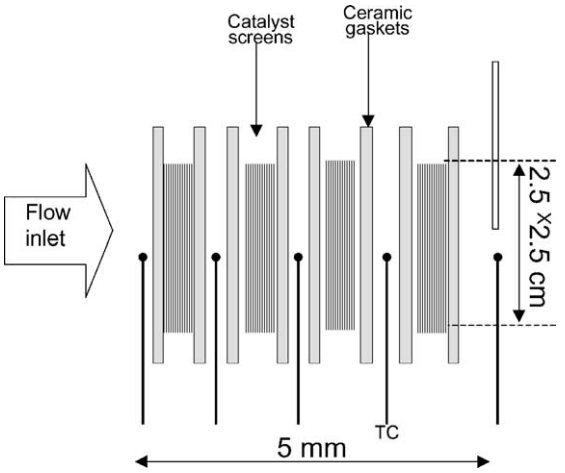

Fig. 6. Schematic diagram of the Microlith® based reactor used in the tests under fuel-lean conditions.

strates discussed above can be employed in controlling the surface temperature during the fuel-lean combustion of methane. Several approaches to designing catalytic reactors for gas turbine applications can be found in literature. In the design, referred to as a hybrid approach, only a portion of the fuel is combusted in the catalytic reactor with combustion completed in a downstream combustor zone [10]. To avoid rapid catalyst degradation in this approach, temperature in the catalytic reactor zone needs to be limited to a value much lower than the adiabatic temperature of the reacting fuel/air mixture. Therefore, limiting the heat release in the catalyst stage while achieving stable and high reaction rate sufficient for adequate preheating of the gas mixture and for stabilizing the downstream flame is one of the greatest challenges of catalytic combustor design.

Testing of the Microlith® substrates for catalytic combustion was performed using a reactor comprised of a series of screens coated with stabilized γ-alumina washcoat and Pd-based catalyst with square frontal area of about 6 cm^2 and a length of ∼0.5 cm, as shown schematically in Fig. 6. Catalyst temperature was measured by thermocouples inserted and compressed between the elements, such that they were in good thermal contact with the catalyst. Several thermocouples equally spaced through the catalyst bed were used to measure the axial temperature profile. The reactor was exposed to a reacting mixture of propylene in air for between 1 and 2 h prior to testing with methane to eliminate any artifacts due to the testing of fresh catalysts samples (in this pre-treatment the last catalyst surface temperature, which was the hottest point in the bed was maintained at ∼750 °C). Both Microlith® reactor behavior and downstream flame combustor performance were investigated. Tests were performed at atmospheric pressure and 500 °C inlet temperature with a mixture of methane and air at equivalence ratios between 0.2 and 0.8 at a space velocity of about $8 \times 10^6\ h^{-1}$, corresponding to residence time of about 0.1 ms.

Fig. 7 shows the performance of the Microlith® catalytic reactor. The inlet gas temperature, inlet, and exit catalyst surface temperatures and exit gas temperature as measured by thermocouples are shown in the plot, while the adiabatic temperature was calculated based on the equivalence ratio of the inlet mixture. It was found that the catalyst temperatures were much lower than the adiabatic flame temperatures at all equivalence ratios. At $\phi = 0.3$ gradual activation of the catalyst was observed, but unlike the usual lightoff process, which occurs almost instantaneously, activation over Microlith® proceeded over a time interval of about 30 min. Catalyst temperature still remained much lower than the adiabatic temperature, which indicates that the reactor is still operating in the kinetically limited regime. Upon further increase in the equivalence ratio the reactor surface temperature did not exceed 800 °C, even at $\phi = 0.8$. Under all tested conditions exit temperature of the gas mixture closely followed catalyst temperature at the end of the bed, which is consistent with extremely high heat transfer coefficient characteristic of the Microlith® substrate. The Microlith® reactor, therefore, demonstrated stable operation over a wide range of operating conditions encountered in gas-turbines, preheating the gas mixture to a desirable temperature of about 800 °C but never exceeding this temperature on the catalyst surface.

The effect of the Microlith® catalytic combustor on flame stabilization was tested by burning the reactor effluent in a downstream combustion zone and measuring emissions downstream of the flame. The combustion zone in this test was essentially a tube with high-temperature ceramic liner and with no additional means for flame stabilization. Emissions data were collected at 500 °C inlet using an emissions rack

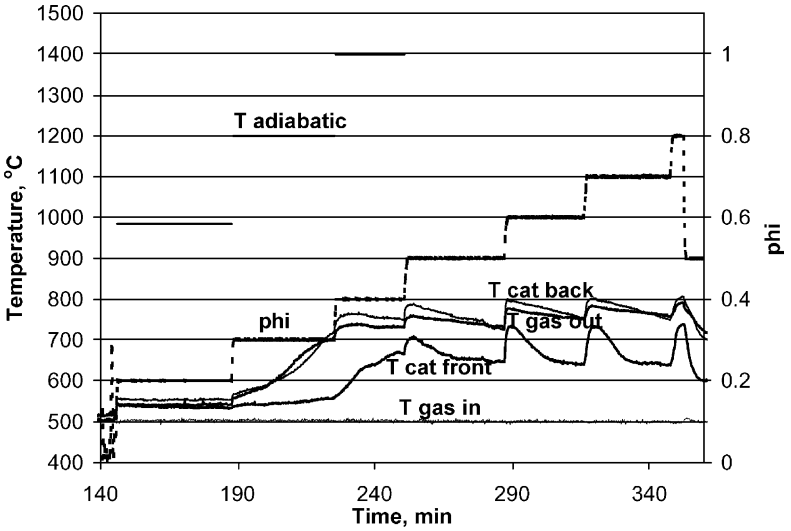

Fig. 7. Microlith® catalytic reactor performance under fuel-lean condition: CH_4 in air, ambient pressure; space velocity, $8 \times 10^6\ h^{-1}$.

equipped with detectors to measure NO_x (Chemiluminescent NO_x Analyzer), hydrocarbons (flame ionization detector), CO (non-dispersive infrared detector), CO_2 (non-dispersive infrared detector) and oxygen (paramagnetic oxygen analyzer). The results of this test are shown in Table 2. Low amounts of CO and UHC even at low equivalence ratio suggest good flame stabilization by the Microlith® catalytic reactor. The amount of NO_x increases with increasing ϕ due to higher flame temperature, but remains below 10 ppm at $\phi = 0.5$. This also suggests good mixing and stable flame combustion.

The results of the Microlith® reactor test shows that a Pd-based catalyst support on short channel length substrates retains steady, controlled performance under conditions where catalyst support on conventional long channel monoliths, operating without additional cooling, would "run away" and likely melt down. We attribute this effect to the combination of high heat transfer rate of the Microlith® substrate and of variation in catalyst activity related to phase transformation of the Pd-based catalyst. This is schematically explained in Fig. 8, which shows a profile of the kinetic rate for methane oxidation over supported Pd catalyst (in units of heat release per unit area) and the upper limits on the reaction rate, which is the mass transfer limited rate, for monolith and Microlith® substrates. Note, that both the kinetic and the mass transfer reaction rates depend on the particular conditions of the test, namely methane concentration, catalyst dispersion, gas mixture flow rate, etc. Therefore, approximate values at some typical reaction conditions are shown in Fig. 8 (note, that the *y*-axis is not to scale). It has been observed that at low temperatures the rate of methane oxidation over the catalyst in PdO state increases with an activation energy of about 70 kJ/mole [11]. However, as the temperature increases to about 750 °C, PdO starts to decompose, which leads to a significant decrease in methane oxidation rate. Once the catalyst is completely reduced, methane oxidation rate over metallic Pd starts to increase again, but at much faster rate (activation energy of about 190 kJ/mole [11]) it may exceed the rate obtained over PdO.

Peak kinetic rate for methane oxidation over supported Pd catalysts can be estimated from the results reported in Ref. [12], where for a lean mixture with 3.2% methane concentration flowing at the volumetric

Table 2
Emissions data from the flame stabilized by Microlith® reactor (normalized to 15% O_2)

ϕ	CO (ppm)	NO_x (ppm)	Total HC (ppm)
0.4	6.3	1.5	1.4
0.45	1.7	3.6	0.3
0.5	1.2	8.3	0.1

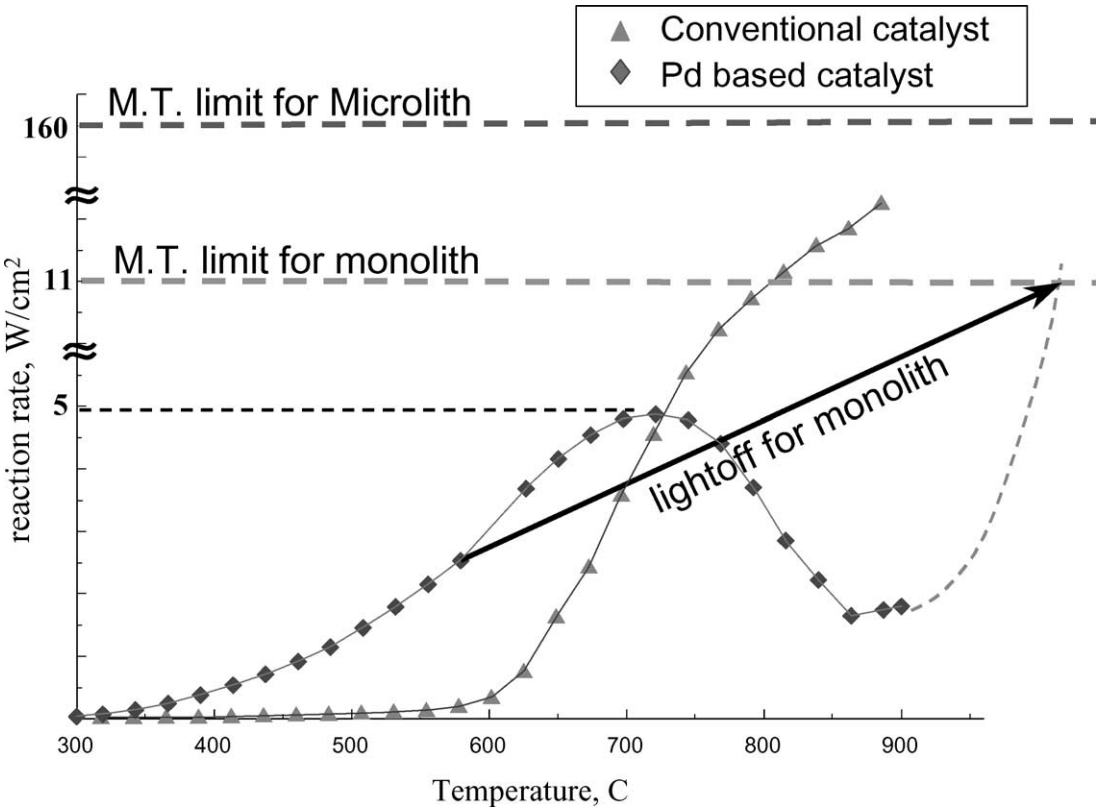

Fig. 8. Qualitative methane oxidation rate over conventional and Pd-based catalyst. Horizontal lines represent mass transfer limit on the reaction rate for a long channel monolith and a Microlith® substrate.

flow rate of about 5 standard liters per minute over a flat plate catalyst strip of 0.64 cm × 1.2 cm, about 4% conversion to CO_2 was measured at 750 °C. This yields the kinetic reaction rate of about 5 W/cm^2. The rate of heat removal from the catalyst surface is determined by the heat transfer coefficient, which is proportional to mass transfer rate and is much higher for Microlith® substrates than for monoliths. The maximum rates of heat removal from the surface for a conventional monolith and for Microlith® substrates are proportional to the mass transfer limited reaction rates, which are represented in Fig. 8 by horizontal lines. Under the conditions of this test for a conventional 1 in. monolith the mass transfer coefficient is about 10 cm/s (see Fig. 3). Then for a gas mixture with 3.2% methane the mass transfer limit on the reaction rate may be estimated to be about 11 W/cm^2. For a Microlith® with $k_g \approx 150$ cm/s (Fig. 4) under the same conditions the mass transfer limit on the reaction rate is about 160 W/cm^2. Therefore, for reaction over a long channel monolith the kinetic reaction rate approaches the mass transfer limit at low temperatures, while the catalyst is in the PdO state. At this point reaction becomes mass transfer limited and catalyst temperature instantaneously jumps to the adiabatic temperature of the gas mixture, which is usually over 1000 °C, as represented by an arrow in Fig. 8. This is consistent with our observations that for conventional long channel monoliths the mass transfer limited reaction condition is reached at a much lower temperature and much lower methane oxidation rate than that obtained for Microlith®. As a result of reaching this mass transfer limited condition, conventional catalysts may “run away” destroying the reactor.

In contrast, mass transfer limited reaction rate over a Microlith® substrate is much higher than the peak

reaction rate over the catalyst in the PdO state. Therefore, the mass transfer limited regime is not reached in the Microlith® reactor and the catalyst temperature stabilizes at the point of peak catalyst activity. If for some reason the catalyst temperature increases beyond this point, the kinetic rate of reaction drops returning surface temperature back to the stable value. Thus specifics of the Pd–PdO transformation in conjunction with enhanced heat and mass transfer rates of the Microlith® substrate provide stabilization of the surface temperature and of the extent of reaction at the desirable level. Oscillations, which are characteristic for Pd-based catalyst supported on long channel monolith substrates (see for example [12]), were not observed over the Microlith®.

4. Application of Microlith® to fuel-rich reforming processes

In another application a Microlith® based reactor was tested for reforming methane into CO and H_2. Similar to the combustion reactor, the reactor used in this test was about 5 mm long and ∼4 cm in diameter and comprised of Microlith® screens coated by stabilized γ-alumina supporting Rh catalyst (Fig. 9). Preheated air was mixed with methane to produce the inlet mixture with equivalence ratio between about three and five at an inlet temperature of about 400 °C. Space

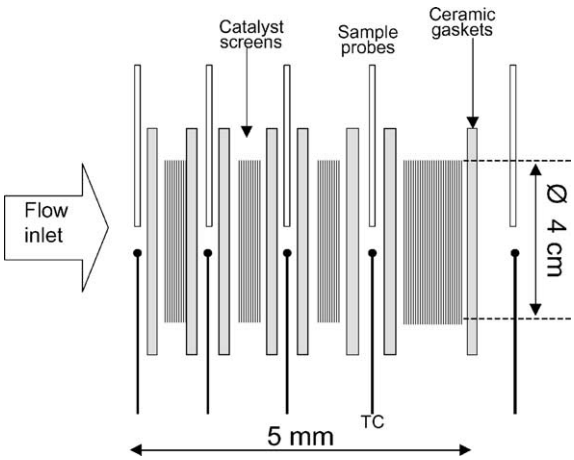

Fig. 9. Schematic diagram of the Microlith® based reactor used in the tests under fuel-rich conditions.

velocity in the reactor was $\sim 10^6\,h^{-1}$, which corresponds to residence time of 0.5 ms. In our tests, up to 90 SLPM of methane could be passed through a reactor having volume of about 10 cm^3. This amount of methane corresponds to a power density of 4 MW per liter of reactor volume.

Thermocouples and gas sample probes were placed along the catalyst bed to measure temperature and gas composition profiles as shown in Fig. 9. Gas samples were pulled by the probes out of the catalyst bed at different axial locations and analyzed by a gas chromatograph. H_2, O_2, N_2, CO, CH_4, and CO_2 concentrations in the mixture were directly measured and water concentration was calculated based on atomic mass balance. Ratio of sum of CO and CO_2 to sum of all carbon species provided methane conversion, while ratio of CO to CO + CO_2 and of H_2 to $H_2 + H_2O$ provided carbon monoxide and hydrogen selectivity, correspondingly.

Temperature and gas composition profiles along the reactor bed are shown in Fig. 10. These data show that all the oxygen is consumed on the very front of the catalyst bed. This leads to a rapid consumption of methane and very high rate of H_2 and CO production. At the point when all the oxygen is consumed, which is less than 1 mm into the catalyst bed, H_2 concentration in the mixture is already about 30% and CO concentration is about 16%. Some CO_2 and H_2O are also produced on the front of the catalyst bed. Note, that the peak concentration of H_2O (∼5%) is much higher than that of CO_2 (∼1%). Apparently, this is due to gas phase oxidation of hydrogen, which is much faster than gas phase oxidation of CO. Rapid oxidation on the front of the catalyst leads to high heat release and high temperatures at the inlet section. The temperature profile measured by thermocouples placed between the Microlith® screens shows that the very front of the bed was the hottest part of the reactor (1050 °C), while the temperature decreased towards the exit of the reactor (∼750 °C). The peak temperature however is below the material limits of the Microlith® substrate and catalyst material and is much lower than peak temperatures usually expected in partial oxidation of methane. After all the oxygen is consumed, the remaining methane is converted in slower, endothermic steam, and CO_2 reforming reactions. This results in further increase in H_2 and CO concentration with decreasing CO_2, H_2O, and CH_4

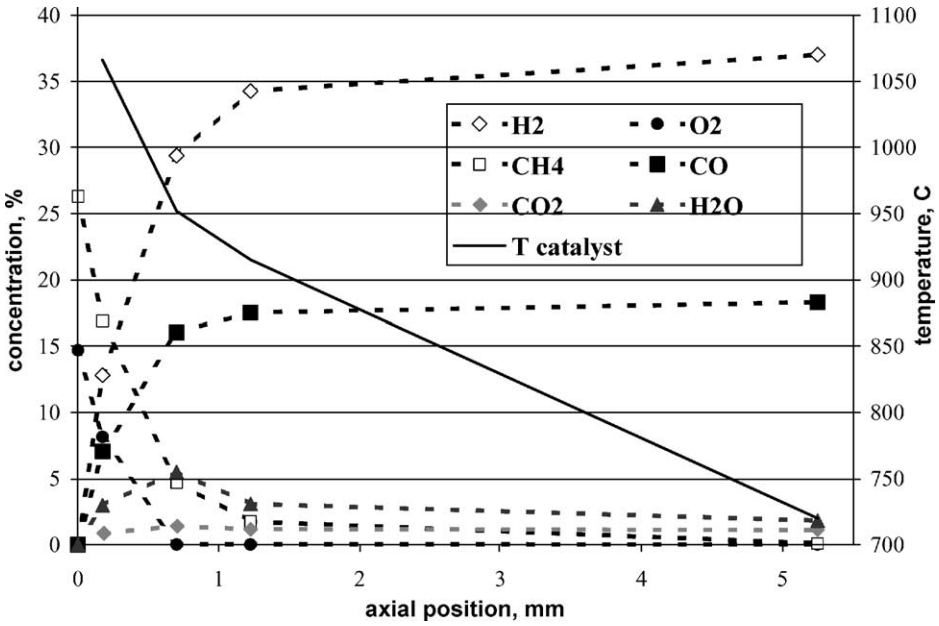

Fig. 10. Temperature and species profile along the Microlith® reactor for partial oxidation of methane into syngas: ambient pressure, $\phi = 3.5$, $v = 2.5$ m/s, and inlet temperature −450 °C.

as well as reactor temperature over the rest of the reactor length, such that thermodynamic equilibrium in the mixture is achieved at the exit of the catalyst bed.

The dependence of the reactor performance on equivalence ratio is shown in Table 3. When the equivalence ratio of the feed mixture is decreased at constant flow velocity, the concentration of H_2 and CO in the product mixture remains almost constant. Increasing the amount of oxygen in the mixture leads to more methane being burnt into CO_2 and H_2O with higher heat release and higher catalyst temperature. Note, though, that essentially complete conversion of methane (99.94%) was achieved in the test with a peak temperature of only 1100 °C. Even under conditions where complete conversion of methane was achieved, process selectivity to partial oxidation products was above 93%.

The dependence of the reactor performance on the inlet flow rate is shown in Table 4. Interestingly, increasing the flow velocity of the feed mixture from 2.7 to 6.4 m/s had very little effect on the process. Methane conversion and process selectivity decreased slightly when the flow velocity was increased by a factor of three, however CO and H_2 concentration in the product mixture remained practically unchanged. Operating the process at the high end of tested flow rates results in production of about 500 kg of syngas per hour per liter of reactor volume and is a major improvement over current steam reforming reactors.

Table 3
Dependence of partial oxidation reaction on the equivalence ratio

ϕ	v (m/s)	T peak (°C)	H_2 (%)	CO (%)	H_2O (%)	CO_2 (%)	CH_4 (%)	Conversion (%)	H_2 selectivity (%)	CO selectivity (%)
4.4	2.6	985	37.65	18.28	0.65	0.87	3.46	84.70	98.30	95.45
4.0	2.6	1028	38.87	18.58	0.15	0.93	0.85	95.82	99.63	95.23
3.4	2.6	1075	36.43	18.22	2.34	1.17	0.06	99.67	93.96	93.96
3.3	2.6	1100	35.65	17.83	2.66	1.33	0.01	99.94	93.06	93.06

Table 4
Dependence of partial oxidation reaction on flow rate

ϕ	v (m/s)	T peak (°C)	H_2 (%)	CO (%)	H_2O (%)	CO_2 (%)	CH_4 (%)	Conversion (%)	H_2 selectivity (%)	CO selectivity (%)
3.5	2.7	992	36.20	18.64	2.87	0.90	0.95	95.36	92.64	95.42
3.4	3.7	1007	35.76	18.90	3.71	0.84	1.00	95.19	90.60	95.76
3.6	5.2	1030	36.34	18.64	2.52	0.79	1.15	94.42	93.51	95.95
3.6	6.4	1048	35.86	18.54	2.75	0.76	1.44	93.07	92.88	96.05

At these high power densities, small pilot size reactors are capable of industrial scale product yield. Further scaling up of such a process is less complicated than it is for traditional chemical reactors as the heat and mass transport issues, which usually are the major challenges in scaling up, are taken into account at the initial stages of reactor development.

To test the catalysts ability to sustain performance under extremely high temperatures observed in the partial oxidation process, a 500 h durability test was performed. Peak temperature and gas composition plots generated in this test are shown in Fig. 11. Because equilibrium gas composition is reached at the reactor exit, which does not depend on variations in the catalyst activity, gas composition from the probe located at the front section of the reactor (at the point where all oxygen had just been consumed) was used to monitor the catalyst activity. Exit gas composition was periodically checked to make sure it did not vary.

The reactor demonstrated stable performance over 500 h. Variations in temperature and gas composition seen in the plot (Fig. 11) are primarily due to rig control artifacts and variations in fuel gas composition. The drop and sharp rise in temperature at about 300 h was due to a large fluctuation in air flow due to a failure of the air compressor control system. The feed mixture composition crossed over stoichiometric value several times before stabilizing at the initial set conditions. Surprisingly this event did not lead to a meltdown of the reactor (consistent with lean methane combustion

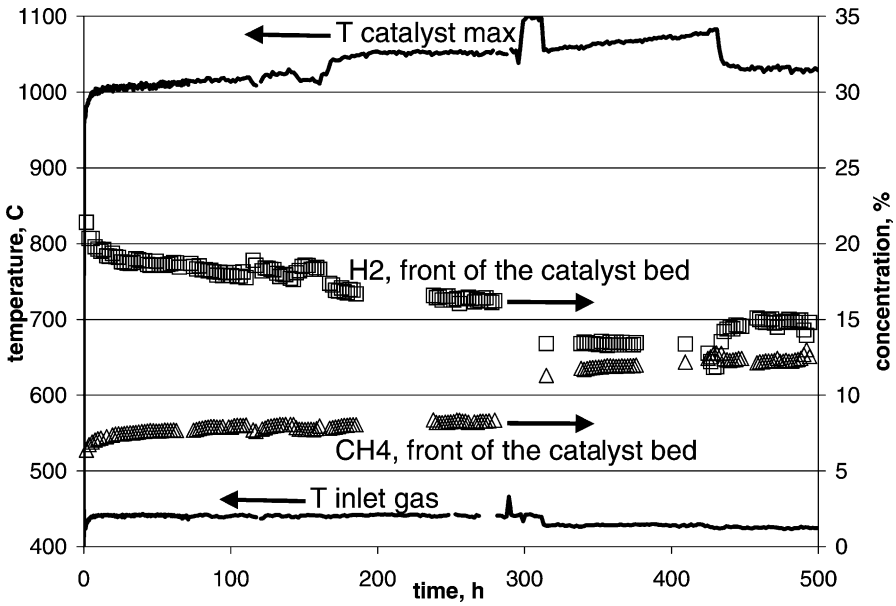

Fig. 11. 500 h durability test over the Microlith® supported catalyst in reaction of partial oxidation of methane to syngas: $\phi = 3.3$ before 330 h, then 3.5; $v = 3.3$ m/s. CH_4 and H_2 concentration is measured by a probe located 0.7 mm from the front of the catalyst bed.

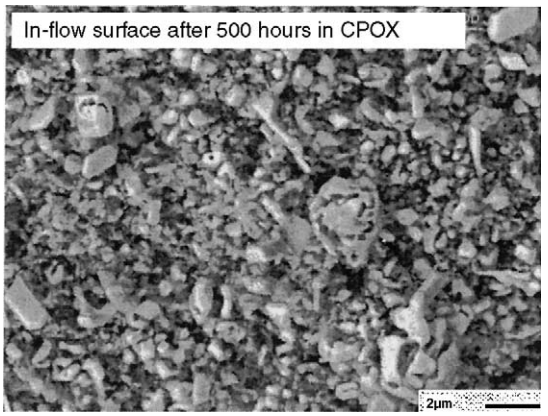

Fig. 12. SEM micrograph of the first Microlith® screen after 500 h test in reaction of partial oxidation of methane into syngas.

experience) or even to severe loss of catalyst activity. A small increase in peak temperature from 1050 to 1100 °C resulted from this controller malfunction. This increase in temperature was later compensated by increasing the equivalence ratio of the mixture from 3.3 to 3.5. This change in the inlet mixture composition caused slight decrease in methane conversion and hydrogen yield, which then remain steady at the new level (Fig. 11). The temperature step at ∼170 h, occurred after switching the reactor feed from pure methane to natural gas (which has fractions of higher hydrocarbons) and the sharp decrease in temperature at ∼430 h was due to switching the feed back to pure methane. The gradual increase in peak temperature from 330 to 430 h was likely due to a slow change in the fuel gas composition, which may be attributed to fractionation of gas components or presence of liquid phase hydrocarbons in the fuel tank (a single tank of gas was used during this period of time). Similar phenomenon of slow drift in catalyst temperature during the prolonged run from a single fuel tank and of sharp change in temperature when switching the tanks was also observed in other similar experiments. This suggests sensitivity of the process to the feed gas composition, with pure methane providing higher selectivity and lower catalyst temperatures than natural gas.

SEM analysis of the sample from the 500 h durability test shown in Fig. 12 indicate that the catalyst had sintered resulting in large, micron-size crystallites covering the whole surface of the substrate. Comparison of the EDS signal from the in-flow and out-of-flow regions of the same screen did not reveal any loss of noble metal, which suggests that restructuring occurred without significant metal vaporization. The washcoat was adherent even in the hottest portions of the reactor. In spite of severe sintering, catalyst performance at the end of the 500 h test remained essentially unchanged and the gas mixture at the exit from the reactor still remained at equilibrium composition. Thus, catalyst life can be safely extrapolated to much longer operation.

Catalytic partial oxidation has been investigated by many groups of researchers both in academia and in industry [13–16]. Controversy about the mechanism of methane partial oxidation to syngas still exists. Schmidt and coworkers [17] argue that methane is directly converted into H_2 and CO; Lunsford and coworkers [13] and Baerns and coworker [18,19] argue that the process goes through a complete oxidation step followed by a reforming step, while Wang and Ruckenstein [20] argue that the mechanism of this process is dependent on the loading of the catalyst and the reaction temperature. In our work, analysis of gas composition on the very front of the catalyst bed, before all the oxygen has been consumed, demonstrated that both partial and complete oxidation products are formed. High levels of CO and H_2 were detected on the very front of the catalyst bed, just after a few Microlith® screens, in the region where the contact time is below 0.1 ms and high concentration of oxygen is still present in the gas phase, suggesting a direct partial oxidation mechanism. Residence time in this region is too short for reforming reactions to be able to produce high amounts of CO and H_2, especially taking into account the low levels of CO_2 and H_2O present on the front of the catalyst bed. On the other hand the initial rise of CO_2 and H_2O concentration in the front section of the reactor followed by their consumption in the back section suggests that some CO and H_2 are also formed through the indirect mechanism.

Apparently, on the front of the reactor both partial oxidation (5) and complete oxidation (6) reactions proceed in parallel. In addition to surface reaction, complete oxidation products can result from gas phase oxidation of CO and H_2 formed in reaction (5):

$$CH_4 + \tfrac{1}{2}O_2 \rightarrow CO + 2H_2 \quad -36\,\text{kJ/mole} \qquad (5)$$

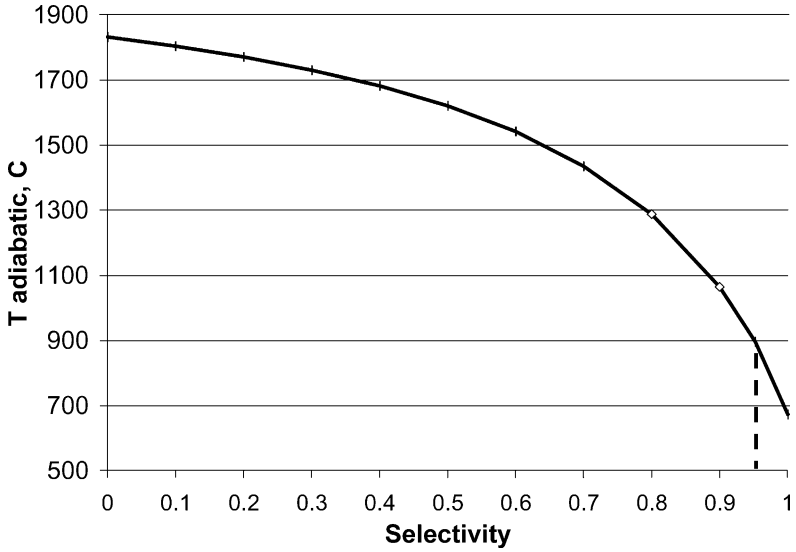

Fig. 13. Correlation between adiabatic temperature and selectivity for partial oxidation of methane (based on thermodynamic calculations for methane/air mixture with equivalence ratio of 3.5 and inlet temperature of 527 °C).

$$CH_4 + 2O_2 \rightarrow CO_2 + 2H_2O \quad -802\,\text{kJ/mole} \qquad (6)$$

Generally speaking, independent of the process occurring at the front of the catalyst bed, reaction products would equilibrate through the rest of the reactor, such that the same final mixture is obtained. It is quite obvious, though, that the indirect mechanism would lead to much higher heat release and much higher temperatures on the front of the catalyst bed, than the direct mechanism. This would result in higher thermal stress and faster degradation of the catalyst.

Dependence of the catalyst temperature on the process selectivity is demonstrated in Fig. 13. Catalytic oxidation reactions are very fast and are mass transfer limited. Under such conditions surface temperature reaches the adiabatic temperature of the gas mixture for the whole length of the catalyst bed [10]. For fuel-lean mixtures adiabatic temperature is uniquely determined by the fuel concentration in air, as only reaction (6) takes place. For fuel-rich mixtures, though, both reactions can proceed simultaneously and adiabatic temperature becomes a function of process selectivity. For a given selectivity (assuming same selectivity for CO and H_2) composition of the product mixture can be found from a mass balance and the adiabatic temperature becomes uniquely determined. The plot shown in Fig. 13 was obtained by thermodynamic calculations of adiabatic temperature rise from the initial mixture of methane and air at $\phi = 3.5$ and $T = 527\,^{\circ}\text{C}$ to the final mixture with composition determined by a given selectivity and complete consumption of the limiting reactant. From the mass balance it can be calculated that achieving complete conversion of methane with 100% selectivity to partial oxidation products is possible only at $\phi = 4.0$. At equivalence ratio of 3.5, the maximum possible selectivity (at which complete consumption of both methane and oxygen occur) is 0.95.

Local selectivity, and therefore adiabatic temperature, on the front of the catalyst bed is determined by the relative rates of reactions (5) and (6) (kinetic selectivity). The discrete nature of the Microlith® substrate suggests low thermal conductivity in the axial direction. Therefore, local surface temperature is determined by local kinetic selectivity of the process rather than by the overall thermodynamic selectivity of the final product. This is also consistent with the high temperature gradients observed in the reactor. From Fig. 13 we find that in order to limit the catalyst temperature at the front end of the reactor to 1100 °C the ratio of the rate of reaction 5 and 6 should be higher than about 0.9 (selectivity of 90%). At lower kinetic

selectivity catalyst temperatures become extremely high such that catalyst loss through volatility becomes a problem even for ceramic substrates which would additionally suffer from extremely high thermal stress.

This analysis suggests that in order to lower the peak temperature in the partial oxidation process complete oxidation reactions should be suppressed and partial oxidation reactions promoted on the front of the catalyst bed. Surface reaction on the catalyst produces partial oxidation products, while gas phase reactions are not selective and can produce high yield of CO_2 and H_2O [17]. Therefore, high rate of reactants transfer to the catalyst combined with high surface area and hence, high activity of the catalyst, which are provided by the Microlith® substrate allow increased rate of partial oxidation reactions relative to the rate of complete oxidation and minimize the catalyst temperature. This provides better thermal efficiency of the process and improved catalyst durability. The ability to run partial oxidation processes at low peak temperatures also allows using mixtures with lower overall equivalence ratios, such that complete conversion of methane could be achieved.

5. Summary

The advantages of the Microlith® catalyst technology are based on the combination of extremely high mass and heat transfer characteristics, high GSA of the substrate and high surface area coatings. These properties of the Microlith® system provide flexibility in designing catalytic reactors and lead to smaller size, lower loading of precious metals and improved performance characteristics.

Application of the Microlith® system with supported Pd-based catalyst to fuel-lean catalytic combustion demonstrated stable performance with the catalyst and exit gas temperatures at about 800 °C over a wide range of inlet conditions. This allowed stabilization of a lean flame downstream of the reactor with simultaneous NO_x, CO, and UHC emissions in a single digit ppm range.

Application of the Microlith® system to fuel-rich partial oxidation of methane allowed decreasing peak temperatures in the reactor to below 1100 °C under the conditions where complete conversion of methane was achieved with 93% selectivity to H_2 and CO. Low peak temperatures in the catalytic bed allow achieving durable reactor operation.

Acknowledgements

We acknowledge the US National Science Foundation's support in conducting a significant portion of this research. Any opinions, findings, and conclusions or recommendations expressed in this publication are those of the authors and do not necessarily reflect the views of the National Science Foundation.

References

[1] S.T. Kolaczkowski, Trans. Inst. Chem. Eng. 73 (1995) 168.
[2] J.R. Sodre, J.A.R. Parise, J. Fluids Eng. 119 (1997) 84.
[3] S. Roychoudhury, J. Bianchi, G. Muench, W.C. Pfefferle, SAE 971023, SAE International, Warrendale, PA, 1997.
[4] J.L. Perry, R.N. Carter, S. Roychoudhury, SAE 1999-01-2112, SAE International, Warrendale, PA, 1999.
[5] G. Kraemer, T. Strickland, W.C. Pfefferle, J. Ritter, in: Proceedings of the International Conference on Joint Power Generation, ASME International, 1997.
[6] U. Ullah, S.P. Waldram, C.J. Bennet, T. Truex, Chem. Eng. Sci. 47 (1992) 2413.
[7] C.N. Satterfield, D.H. Cortez, Ind. Chem. Fundam. 9 (1970) 613.
[8] R.K. Shah, A.L. London, Laminar flow forced convection in ducts, in: Advances in Heat Transfer, Academic Press, New York, 1978.
[9] R.N. Carter, S. Roychoudhury, W. Pfefferle, G. Muench, H. Karim, Proceedings of the MRS Symposium, vol. 454, Materials Research Society, 1997 .
[10] L.D. Pfefferle, W.C. Pfefferle, Catal. Rev.-Sci. Eng. 29 (2–3) (1987) 219–267.
[11] M. Lyubovsky, L. Pfefferle, Catal. Today 47 (1999) 29–44.
[12] M. Lyubovsky, L. Smith, M. Castaldi, H. Karim, B. Nentwick, S. Etemad, R. LaPierre, W.C. Pfefferle, Catal. Today, this issue.
[13] D. Dissanayake, M.P. Rosynek, K. Kharas, J.H. Lunsford, J. Catal. 132 (1991) 117.
[14] D.A. Hickman, E.A. Haupfear, L.D. Schmidt, Catal. Lett. 17 (1993) 223.
[15] Y. Fujitani, H. Muraki, US Patent 4,087,259 (1978).
[16] L.L.G. Jacobs, P.W. Lednor, A.G.G. Limahelu, R.J. Schoonebeek, K.A. Wonkeman, US Patent 5,510,056 (1996).
[17] C.T. Goralski Jr., R.P. O'Connor, L.D. Schmidt, Chem. Eng. Sci. 55 (2000) 1357.
[18] O.V. Buyevskaya, K. Walter, D. Wolf, M. Baerns, Catal. Lett. 38 (1996) 81.
[19] O.V. Buyevskaya, D. Wolf, M. Baerns, Catal. Lett. 29 (1994) 249.
[20] H.Y. Wang, E. Ruckenstein, J. Phys. Chem. B 103 (1999) 11327.